

DOI:10.1002/ejic.201402123

Sonogashira, CuAAC, and Oxime Ligations for the Synthesis of Mn^I Tricarbonyl PhotoCORM Peptide Conjugates

Sandesh Pai,^[a] Krzysztof Radacki,^[a] and Ulrich Schatzschneider*^[a]

Keywords: Bioinorganic chemistry / CO release / Bioorthogonal coupling / Peptides / Carbonyl ligands / Manganese

In this work, facial tricarbonylmanganese(I) complexes [Mn(bpea^{CH₂C₆H₄R})(CO)₃]PF₆ incorporating a functionalized 2,2-bis(pyrazolyl)ethylamine (bpea) ligand with R = I, C≡CH, and CHO have been explored for their utility in bioorthogonal coupling to carrier peptides bearing *N*-terminal alkyne, azide, and aminoxy residues. As a model system, the transforming growth factor β-recognizing (TGF-β) peptide sequence R'-Leu-Pro-Leu-Gly-Asn-Ser-His-OH was used in which R' is the reactive group complementary to the metal complex functionality. The use of catalyst-free oxime ligation

gave the most stable conjugate with no degradation observed by HPLC over 96 h even after repeated freeze–thaw cycles. Both the parent complex as well as the functionalized peptide were investigated for photoactivated CO delivery to heme proteins by using the myoglobin assay and found to have essentially identical release properties. This work has established a new strategy for the conjugation of photoactivatable CO-releasing molecules (PhotoCORMs) to biological carrier systems.

Introduction

It is now well established that carbon monoxide, endogenously produced by the action of heme oxygenase (HO) enzymes on heme,^[1] has a very important biological function in higher organisms, including humans, in particular in the context of small-molecule signaling and protection against oxidative stress.^[2–5] During the last decade, methods to intervene in these CO-modulated biochemical processes for potential therapeutic applications in human medicine have gained steadily increasing attention. Whereas the controlled application of CO gas by inhalation is of limited use only due to the fixed partition ratio between lungs, blood, and different tissues, making a selective targeting of specific diseased structures in the body difficult, organic and organometallic compounds have been developed as prodrug carrier systems for carbon monoxide, for which the term “CO-releasing molecules” (CORMs) was coined by Motterlini and co-workers.^[6–11] A wide range of metal carbonyl co-ligand structures have been explored for their utility as CORMs, and different trigger mechanisms are now well established to initiate the release of CO from the metal coordination sphere. In addition to simple ligand exchange reactions with solvent or the constituents of biological systems,^[12] they

also include the action of esterase and phosphatase enzymes on carbonylmetal complexes (enzyme-triggered CORMs, ET-CORMs),^[13–16] the use of magnetothermal heating in an alternating electrical field,^[17] and the use of light to stimulate the liberation of CO (PhotoCORMs).^[18–21] Only more recently the focus of the field has shifted from the simple introduction of an ever-increasing number of novel metal carbonyl core structures as CORMs to a proper design of the whole system to really turn these compounds into viable drug candidates. As nicely outlined by Romao et al., in addition to the so-called inner CORM sphere, which controls the stoichiometry and kinetics of CO release, special attention must also be paid to the drug sphere, the outer ligand periphery of a carbonylmetal complex, which determines its distribution and uptake in different tissues and cells.^[22] By very careful selection of functionalized isocyanato ligands coordinated to a molybdenum(0) tricarbonyl core, for example, it has been possible to achieve very selective liver accumulation to alleviate the toxic effects of acetaminophen-induced severe acute liver injury.^[23] As an alternative to the design of small-molecule CO prodrugs, the conjugation of established CORMs to macromolecules as well as hard and soft nanomaterials for the targeted delivery of carbon monoxide has also been explored. In addition to CO- and CORM-loaded micelles and metal–organic frameworks (MOFs),^[24,25] carbon- and silica-based nanoparticles have also been decorated with CO-releasing molecules by using the CuAAC click reaction.^[26,27] A particular focus has been on carrier peptides for the targeted delivery of CORMs,^[28] because solid-phase peptide synthesis (SPPS) allows a facile variation of the amino acid sequence and thus modulation

[a] Institut für Anorganische Chemie, Julius-Maximilians-Universität Würzburg, Am Hubland, 97074 Würzburg, Germany
E-mail: ulrich.schatzschneider@uni-wuerzburg.de
http://www-anorganik.chemie.uni-wuerzburg.de/en/research/prof_dr_u_schatzschneider

Supporting information for this article is available on the WWW under <http://dx.doi.org/10.1002/ejic.201402123>.

of the cellular and tissue accumulation. In addition to cell-penetrating peptides,^[29] which are generally capable of membrane transition, there are also peptides that are more specifically recognized by complementary binding partners. Although robust organometallic half-sandwich complexes can be directly conjugated to a growing peptide chain during SPPS by amide bond formation,^[30–36] most CORMs are not stable under the standard conditions for cleavage from the solid support and thus require a post-labeling strategy by bioorthogonal coupling reactions.^[37–40] So far, our work has mostly relied on palladium-mediated Sonogashira coupling and copper-catalyzed azide–alkyne cycloaddition (CuAAC) reactions,^[26,27,41] which are, however, limited in scope due to the use of a potentially toxic transition-metal catalyst. Thus, in this paper, we report on the facile synthesis of a novel aldehyde-functionalized tridentate ligand and the use of its tricarbonylmanganese(I) complex in oxime ligation to an aminoxy-functionalized transforming growth factor β -recognizing (TGF- β) peptide.^[42] This very mild and catalyst-free conjugation method^[43–45] is contrasted with more conventional Sonogashira- and CuAAC-based procedures and is shown to give excellent results in terms of conjugate accessibility and stability.

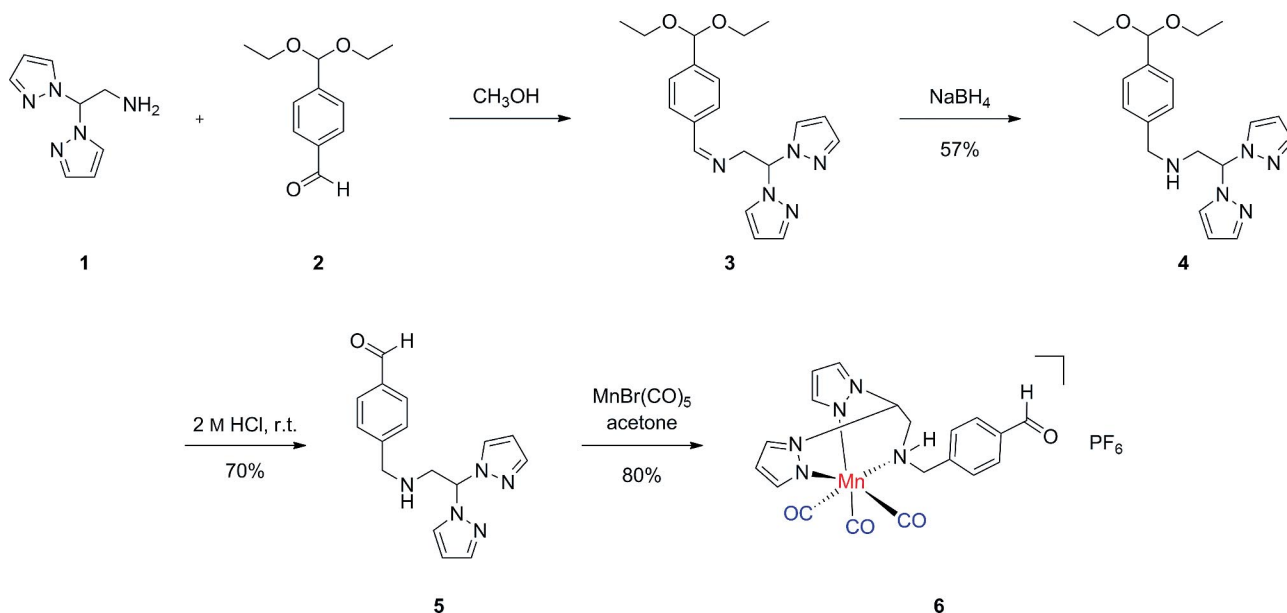
Results and Discussion

Synthesis and Spectroscopic Characterization

We recently introduced the 2,2-bis(pyrazolyl)ethylamine (bpea) ligand into the field of CO-releasing molecules (CORMs) due to its facile functionalization at the primary amino group by condensation with substituted aldehydes. In particular, benzaldehyde derivatives give rise to quite stable imine adducts, which can be further converted by sodium borohydride reduction into the corresponding second-

ary amines, giving very stable pendant functionalization. Although the 4-iodobenzyl and 4-ethynylbenzyl bpea ligands required for Sonogashira and CuAAC coupling have already been reported in previous work,^[46] the corresponding aldehyde-functionalized ligand was still missing from our arsenal. To prevent the formation of 1,4-disubstituted byproducts and allow selective reduction of the imine in the presence of the aldehyde group, bpea^{NHCH₂C₆H₄CHO} (**5**) was synthesized starting from 2,2-bis(pyrazolyl)ethylamine (**1**), which was first condensed with 4-(diethoxymethyl)benzaldehyde (**2**) and then, without isolation of the imine **3**, reduced with sodium borohydride in methanol to give **4** (Scheme 1). Removal of the acetal protective group with 2 M hydrochloric acid gave the desired ligand **5** in 70% yield as a yellow oil. Reaction of **5** with pentacarbonylmanganese bromide in acetone at reflux under nitrogen and the exclusion of light then afforded the corresponding facial tricarbonylmanganese(I) complex **6** in 80% yield as a yellow solid upon precipitation with aqueous potassium hexafluorophosphate. The two related complexes [Mn(bpea^{N=CHC₆H₄I})(CO)₃]PF₆ (**7**) and [Mn(bpea^{N=CHC₆H₄C \equiv CH})(CO)₃]PF₆ (**8**), incorporating an iodo- or alkyne-functionalized bpea ligand, respectively, were available by a similar procedure described in previous work.^[46]

The ¹H and ¹³C NMR as well as IR spectra of the new ligand **5** are in full accordance with the expected structure. The ATR IR spectrum of complex **6** shows two strong bands at 2036 and 1928 cm⁻¹, as expected for C_{3v} symmetry, assigned to symmetrical and antisymmetrical C=O stretching vibrations, respectively. An additional peak at 1691 cm⁻¹ is due to the C=O vibrational band of the aldehyde functional group (Figure 1). In addition, coordination to the metal center leads to a shift in the methine proton signal in the ¹H NMR spectrum from δ = 6.55 to 7.47 ppm. Furthermore, the methylene protons at the α position with respect



Scheme 1. Synthesis of [Mn(bpea^{NHCH₂C₆H₄CHO})(CO)₃]PF₆ (**6**) for catalyst-free oxime ligation.

to the coordinated amine group now each appear as a doublet at $\delta = 3.57$ and 3.18 ppm with 2J coupling constants of 13.2 and 13.8 Hz, respectively, indicative of the diastereotopic environment generated by metal complexation. The signals are both further split by coupling with the adjacent methine and NH protons (see Figure S1 in the Supporting Information). The positive-mode ESI mass spectrum shows one signal at $m/z = 434.08$, which is assigned to the cationic $[M - PF_6]^+$ unit of complex **6**, and an additional one at $m/z = 350.09$ due to the species $[M - 3 CO - PF_6]^+$ (see Figure S2).

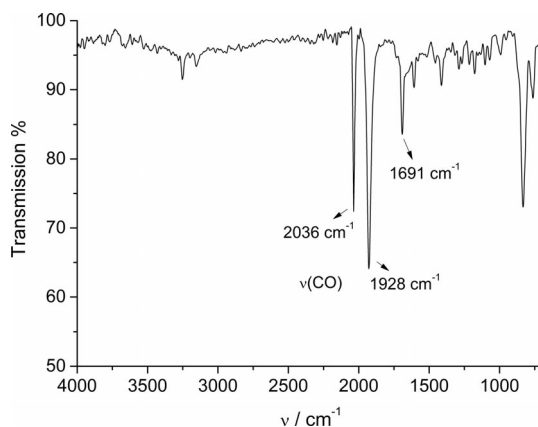


Figure 1. ATR IR spectrum of $[Mn(bpea^{NHCH_2C_6H_4CHO})(CO)_3]PF_6$ (**6**).

X-ray Crystallography

Crystals of **6** suitable for X-ray structure analysis were obtained by recrystallization from dichloromethane/diethyl ether at room temperature. The crystallographic parameters are summarized in Table 1, and the molecular structure is shown in Figure 2. The compound crystallizes in the monoclinic space group $P2_1/n$. The Mn^I center is bound to three

CO ligands in a facial arrangement with the three nitrogen donor groups from the bpea ligand completing the octahedral coordination environment and the 4-formylbenzyl group pointing away from the metal center. Although the distances between the Mn center and the two pyrazolyl N donor atoms of $2.032(2)$ and $2.047(2)$ Å are shorter by about 0.11 Å than the third manganese–amine N bond length of $2.151(2)$ Å, the Mn–C and C≡O bond lengths show essentially no variation with the nature of the *trans* N ligand.

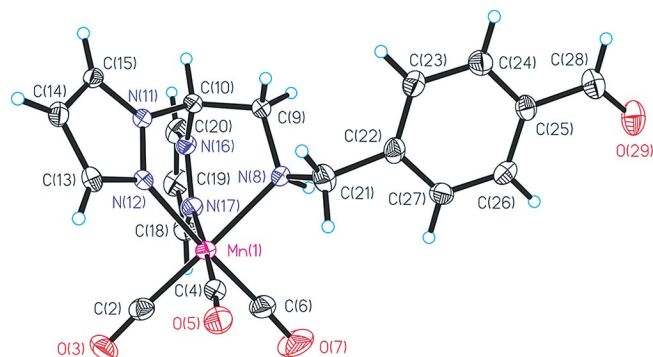


Figure 2. Molecular structure of the cationic unit of **6** with thermal ellipsoids drawn at the 50% probability level. The hexafluorophosphate counter ion is not shown for clarity. Selected bond lengths [Å] and angles [°]: Mn–C(2) 1.813(3), Mn–C(4) 1.817(3), Mn–C(6) 1.811(3), Mn–N(8) 2.151(2), Mn–N(12) 2.032(2), Mn–N(17) 2.047(2), C(2)–O(3) 1.147(4), C(4)–O(5) 1.146(4), C(6)–O(7) 1.141(4), C(28)–O(29) 1.219(4); C(2)–Mn–C(6) 88.22(14), C(4)–Mn–C(6) 90.24(14), C(2)–Mn–C(4) 87.87(13), N(12)–Mn–N(17) 87.29(9), N(8)–Mn–N(12) 84.95(9), N(8)–Mn–N(17) 82.70(9), C(6)–Mn–N(8) 91.68(12), C(2)–Mn–N(8) 174.31(12), C(4)–Mn–N(8) 97.82(12), C(6)–Mn–N(12) 176.57(12), C(2)–Mn–N(12) 95.20(11), C(4)–Mn–N(12) 89.63(11), C(6)–Mn–N(17) 92.89(13), C(2)–Mn–N(17) 91.62(12), C(4)–Mn–N(17) 176.82(11).

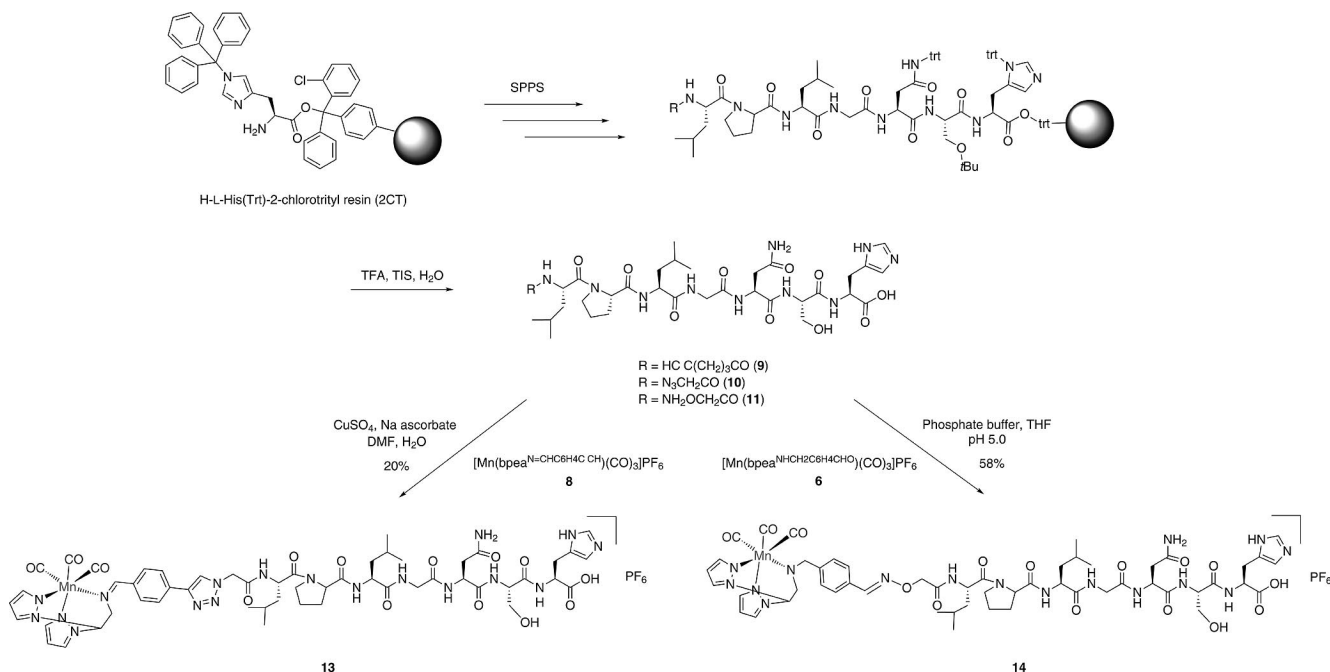
Bioorthogonal Conjugation and Characterization of Peptide Conjugates

For the synthesis of the PhotoCORM peptide conjugates, three different bioorthogonal coupling methods were evaluated. In all cases the amino acid sequence R'-LPLGNSH-OH was used^[47] derived from a TGF β_1 -binding peptide with R' being a suitable N-terminal building block for the coupling with the bpea ligand bearing the complementary coupling partner. Whereas metal complex **7** – incorporating an iodobenzyl group on the bpea ligand – was to be used in a Sonogashira reaction, the alkyne-functionalized analogue **8** is suitable for CuAAC coupling. In addition, new aldehyde-modified ligand **5** and its manganese(I) complex **6** were synthesized for oxime ligation to the peptide.^[45] The peptide sequence was assembled by solid-phase peptide synthesis (SPPS) on a preloaded H-L-His(Trt)-2CT resin by using standard Fmoc methodology. Then, N-terminal functionalization with 5-hexynoic acid, 2-azidoacetic acid, or (aminoxy)acetic acid was carried out on the resin using identical methodology, followed by con-

Table 1. Crystallographic parameters for complex **6**.

Empirical formula	$C_{19}H_{17}F_6MnN_5O_4P$
M_r	579.29
Dimensions [mm]	$0.14 \times 0.12 \times 0.05$
Space group	$P2_1/n$
a [Å]	15.0215(14)
b [Å]	9.2082(11)
c [Å]	16.4618(14)
β [°]	91.226(5)
V [Å ³]	2276.5(4)
Z	4
$\rho_{\text{calcd.}}$ [g cm ⁻³]	1.690
T [K]	100(2)
μ [mm ⁻¹]	0.737
λ [Å] (Mo- K_α)	0.71073
$2\theta_{\text{max}}$ [°]	27.50
Reflections measured	4492
Unique reflections [$I > 2\sigma(I)$]	3560
Variables	307
$R1^{[a]}$ ($I \geq 2\sigma$)	0.0424
$wR2^{[b]}$ ($I \geq 2\sigma$)	0.0972

[a] $R1 = \sum |F_o| - |F_c| / \sum |F_o|$. [b] $wR2 = \{\sum [w(F_o^2 - F_c^2)^2] / \sum [w(F_o^2)^2]\}^{1/2}$.



Scheme 2. Synthesis of peptide conjugates **13** and **14** by CuAAC and catalyst-free oxime ligation.

jugation to **6–8**. The peptides were cleaved from the solid support with a cocktail of TFA/TIS/H₂O (90:5:5), with TIS = triisopropylsilane, and purified by preparative HPLC when necessary to give peptides **9–11** (Scheme 2). The peptides were obtained in high purity (97%) and in yields of 55–60%. Then Sonogashira coupling of **7** with the hexynoic acid terminated peptide **9** was investigated under different standard conditions by using [PdCl₂(PPh₃)₂] as catalyst and copper(I) iodide as co-catalyst.^[48–50] However, despite repeated attempts with different modifications of the reaction conditions, no conjugate **12** could be detected in any case, as monitored by ESI-MS and HPLC. Therefore, we turned to the CuAAC “click” reaction between alkyne-functionalized complex **8** and the azidoacetic acid modified peptide **10**, which was carried out in DMF/water (1:1, v/v) using copper(II) sulfate as the catalyst and sodium ascorbate as the in situ reductant to generate the active copper(I) species (Scheme 2). The resulting product was analyzed by HPLC and showed one main peak with a retention time of 30.1 min, which is significantly longer than that of peptide **10**, for which $t_R = 22.9$ min (Figure 3). Further proof of the successful CuAAC coupling, which leads to a triazole linkage between the metal complex and the peptide, came from ESI-MS. For peptide **10**, a major peak is observed at $m/z = 820.40$, which is due to $[M + H]^+$ (see Figure S3 in the Supporting Information). Conjugate **13**, on the other hand, shows one peak arising from a monocationic species at $m/z = 1247.45$, assigned to $[M - PF_6]^+$, in addition to peaks from dicationic species at $m/z = 624.23$ and 582.24 , due to $[M - PF_6 + H]^{2+}$ and $[M - 3 CO - PF_6 + H]^{2+}$, respectively (see Figure S4). The ATR IR spectrum of conjugate **13** also shows two bands at 2040 and 1932 cm⁻¹, indicative of the incorporation of the intact tricarbonylmetal moiety into the

peptide (see Figure S5). However, it proved difficult to isolate the modified peptide in high purity, because repeated preparative HPLC never gave a completely pure product.

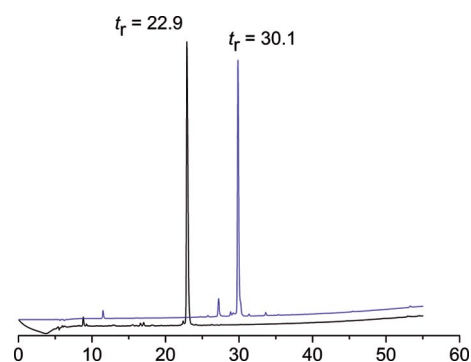


Figure 3. Analytical HPLC chromatogram of peptide **10** (black, 220 nm) and conjugate **13** (blue, 350 nm) after purification by preparative HPLC.

Therefore, we analyzed the stability of conjugate **13** by analytical HPLC in acetonitrile/water (10:90, v/v). In addition to the initial major peak at $t_R = 30.1$ min, a second signal with a slightly shorter retention time of 27.6 min gradually grew in and reached an intensity of 30% relative to the major peak after 39 h (Figure 4). This slow decomposition of the conjugate is presumably due to hydrolysis of the imine bond in the bpea part of the ligand under these conditions.

Therefore, as an alternative method, we turned to oxime ligation, which proceeds under mild and catalyst-free conditions to give very stable conjugation products and also mitigates problems of purification due to co-reactants. In ad-

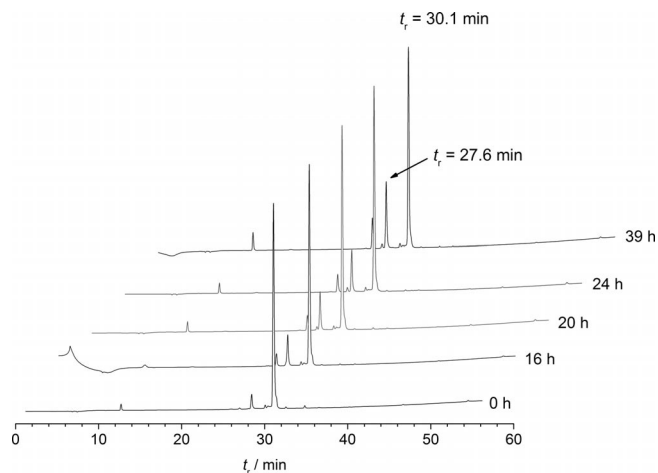


Figure 4. Normalized HPLC traces (350 nm detection) of peptide conjugate **13** upon incubation in acetonitrile/water (10:90, v/v) recorded at room temperature over 39 h.

dition, the bpea ligand was modified to incorporate a more stable secondary amine as in **6** instead of the imine linkage in **8** between the bis(pyrazolyl) moiety and the rest of the ligand (Scheme 1). For the coupling, (aminoxy)acetic acid (Aoa) was attached to the *N*-terminus of the peptide sequence through solid-phase peptide synthesis (SPPS), as described earlier (Scheme 2).^[44] Two repeated couplings with 10 equiv. of Fmoc-Aoa-OH were required to give a negative Kaiser test. Peptide **11** was obtained as a white solid in 60% yield after purification by preparative HPLC. Analytical HPLC showed a high purity (97%) of the product with a retention time of 15.6 min. Further characterization by ESI-MS gave only a single major peak at $m/z = 810.41$, assigned to $[M + H]^+$ (Figure 5).

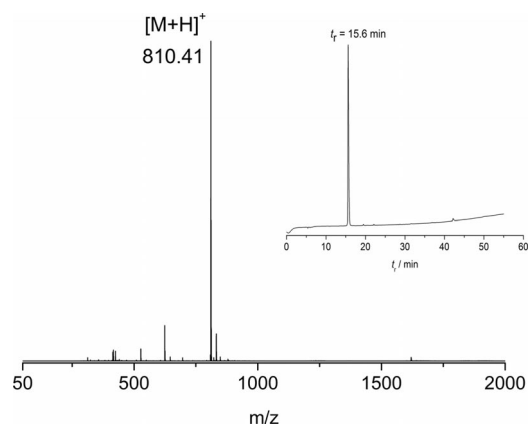


Figure 5. ESI⁺ mass spectrum and analytical HPLC chromatogram (inset) of peptide **11** (220 nm detection).

For the conjugation, Aoa-functionalized peptide **11** was treated with $[\text{Mn}(\text{bpea}^{\text{NHCH}_2\text{C}_6\text{H}_4\text{CHO}})(\text{CO})_3]\text{PF}_6$ (**6**) in a mixture of tetrahydrofuran/phosphate buffer (1:1, v/v) at pH 5.0 at room temperature for 3 h (Scheme 2). The mixture was desalted on a short reversed-phase column (C₁₈-SepPak) and subsequently purified by preparative HPLC.

Peptide conjugate **14** was obtained in moderate yield (58%) but with an excellent purity of 98%. Analytical HPLC of the product showed a significantly longer retention time with respect to peptide **11** with $t_R = 28.3$ min. In the ESI mass spectrum, two main signals from monocationic species are found at $m/z = 1225.45$ and 435.65 , which correspond to the conjugate $[\text{M} - \text{PF}_6]^+$ and a fragment peak resulting from cleavage of the oxime linkage assigned to $[\text{Mn}(\text{bpea}^{\text{CHO}})(\text{CO})_3 + \text{H}]^+$, respectively (Figure 6). The successful conjugation of the complex to the peptide is also evident from the two strong $\text{C}\equiv\text{O}$ vibrational bands in the IR spectrum at 2042 and 1935 cm^{-1} (see Figure S6 in the Supporting Information).

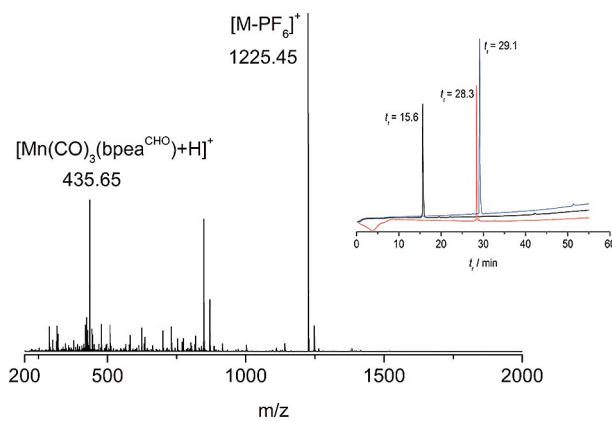


Figure 6. Positive-mode ESI mass spectrum of conjugate **14** and (inset) overlay of analytical HPLC chromatograms of metal complex **6** (blue, 350 nm), peptide **11** (black, 220 nm), and peptide conjugate **14** (red, 350 nm).

Stability Studies in DMSO and Water

To gain an insight into the stability of the novel (bpea) tricarbonylmanganese(I) complex **6** and its peptide conjugate **14**, UV/Vis spectroscopy studies were carried out. Owing to the poor water solubility of complex **6**, it was dissolved in dimethyl sulfoxide. No spectral changes could be observed over a period of 16 h when the compound was kept in the dark. Illumination at 365 nm with a UV hand lamp, coincident with the MLCT absorption maximum of the $\text{Mn}(\text{bpea})(\text{CO})_3$ moiety, however, led to a quick fading of the main absorption band at 357 nm (Figure 7 and Figure S7 in the Supporting Information). The stability of the peptide conjugate **14**, on the other hand, was more conveniently investigated by using RP-HPLC in pure water. HPLC traces were recorded after repeated freeze–thaw cycles ($-25\text{ }^\circ\text{C}$ to room temperature) under the exclusion of light and showed no signals other than the main peak of the conjugate at $t_R = 28.3$ min, which could be observed unaltered over the course of 4 d (Figure 8) and indicates the excellent dark stability of both the $\text{Mn}(\text{CO})_3$ moiety with the reduced amine ligand **5** as well as the oxime linkage to the peptide.

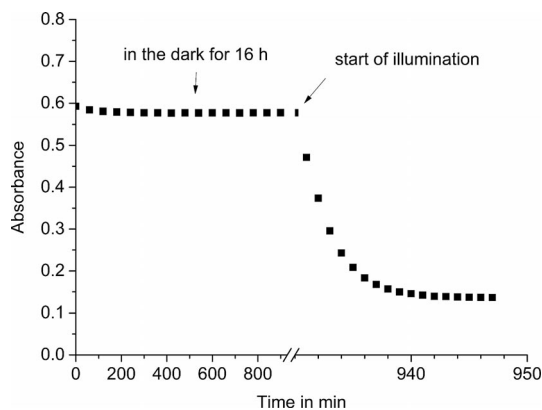


Figure 7. Changes in the absorbance of **6** at 357 nm upon incubation in dimethyl sulfoxide in the dark for up to 16 h and during subsequent photolysis of the same solution with an UV hand lamp at 365 nm. See Figure S7 for the full spectral traces.

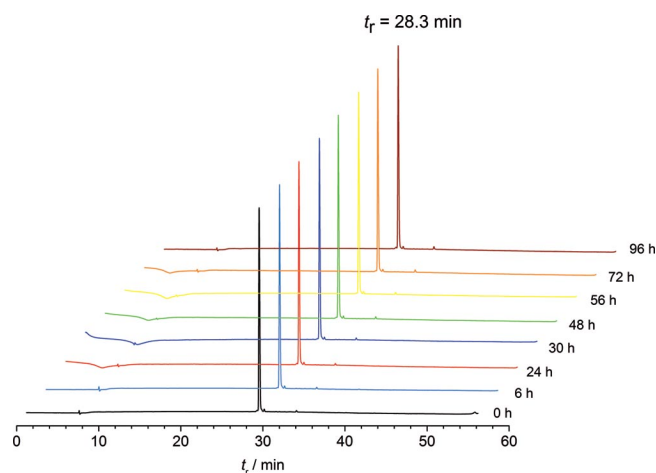


Figure 8. Normalized HPLC traces (350 nm detection) of peptide conjugate **14** upon incubation in water for a period of up to 96 h. The conjugate was dissolved in water, and HPLC traces were recorded after repeated freeze–thaw cycles (–25 °C to room temperature) under the exclusion of light.

CO Release Measurements by the Myoglobin Assay

The standard myoglobin assay was used to compare the CO release behavior of both the parent complex **6** and the peptide conjugate **14**, exploiting the conversion of deoxy-Mb into carbonmonoxy-Mb.^[51,52] A freshly prepared buffered aqueous solution of horse skeletal myoglobin (MbFe^{II}) was reduced with sodium dithionite solution under nitrogen. Incubation in the dark for up to 16 h under the conditions of the myoglobin assay did not lead to any noticeable changes in the Q-band region of the UV/Vis

spectrum (Figure 9 and Figures S8 and S9 in the Supporting Information), which indicates that both the parent complex and the conjugate are stable under these experimental conditions. Thus, both compounds act as dark-stable prodrugs for phototriggered CO release. Only upon illumination at 365 nm were characteristic changes in the UV/Vis spectra noted that are indicative of the conversion of MbFe^{II} (deoxy-Mb) with $\lambda_{\text{max}} = 557$ nm into MbFe^{II}CO (carboxy-Mb) with $\lambda_{\text{max}} = 540$ and 577 nm (see Figure S10). The concentration of the MbFe^{II}CO formed was calculated by using a molar extinction coefficient of $\epsilon_{540} = 15.4 \text{ mm}^{-1} \text{ L}^{-1}$.^[6] Approximately 2 equiv. of CO were released per molecule of either **6** or **14** (Figure 9 and Figures S11 and S12). The CO release data with the half-lives of both the complex and the conjugate are presented in Table 2. Differences in the CO release parameters between both compounds are small and probably due to difficulties in the accurate preparation of stock solutions of the peptide conjugate due to its highly hygroscopic nature.

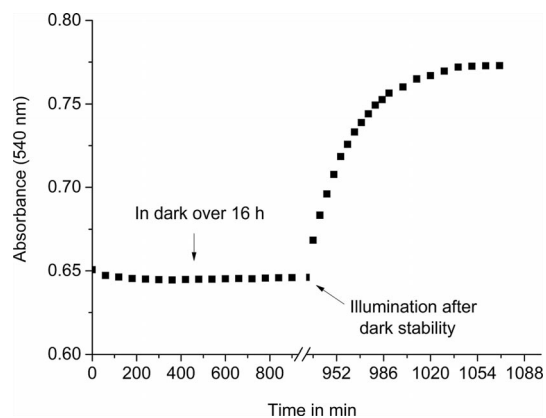


Figure 9. Change in absorption at 540 nm showing the stability of complex **6** (15 μM) in the dark (over the course of 16 h) and the formation of MbCO upon illumination at 365 nm in 0.1 M PBS at pH 7.4 in the presence of myoglobin (60 μM) and sodium dithionite (10 mM) under nitrogen.

Quantum Yield Determination

Standard ferrioxalate actinometry was used to determine the quantum yield of the CO release reaction. The quantum yields (Φ) for both the complex and the conjugate are listed in Table 2 and are in the order of 10^{-4} . These Φ values were calculated from the initial spectral changes and are much lower than those of other carbonylmetal complexes such as $\text{Na}_3[\text{W}(\text{CO})_5(\text{TPPTS})]$ ^[53] and $[\text{Mn}(\text{tpa})(\text{CO})_3]\text{ClO}_4$.^[54,55] Nonetheless, it should be taken into account that these ex-

Table 2. CO release data and quantum yields at 365 nm (Φ_{365}) for **6** and **14**.

Compound	[MbCO] [μM]	CO released [equiv.]	$t_{1/2}$ ^[a] [min]	k_{CO} ^[b] [10^{-4} s^{-1}]	Φ_{365} ^[c] [10^{-4}]
6	30.71 ± 0.40	2.06 ± 0.03	22.58 ± 0.33	5.5	4.36 ± 0.03
14	25.05 ± 0.01	1.70 ± 0.08	15.51 ± 0.52	7.4	4.52 ± 0.14

[a] Under the conditions of myoglobin assay. [b] In DMSO solution from UV/Vis spectra. [c] Calculated by using a photon flux of the UV hand lamp $(2.82 \pm 0.05) \times 10^{-8} \text{ Einstein s}^{-1}$.

periments were performed under the conditions of the myoglobin assay rather than in pure solvent with the protein showing a significant internal shielding effect at the excitation wavelength of 365 nm.^[56,57]

Conclusions

In this work we used the facile functionalization of the bpea ligand framework to introduce three different groups into the periphery of the complex that are suitable for bio-orthogonal coupling reactions, namely iodine for Sonogashira coupling with alkyne-terminated peptides, an alkyne for the CuAAC click reaction with azidoacetic acid modified peptides, and a *p*-benzaldehyde group for oxime ligation with (aminoxy)acetic acid functionalized systems. Under the different conditions examined, we could not obtain a coupling product by the Sonogashira reaction with complex **7**, but complexes **6** and **8** gave the corresponding carbonylmetal complex peptide conjugates linked through either an oxime or triazole linker. It turned out that not only the coupling methodology is vital for successful conjugation, but also the bpea ligand structure. Whereas the imine-based ligand showed slow hydrolysis in acetonitrile/water over the course of 1–2 d, the corresponding amine compound, when combined with the oxime linker, was highly stable for up to 96 h, even under repeated freeze–thaw cycles. Both the parent complex and the peptide conjugate are CO prodrugs when kept in the dark, but release up to 2 equiv. of carbon monoxide upon photoactivation. Thus, this work has allowed the facile, catalyst-free preparation of CORM-peptide conjugates for the targeted delivery of carbon monoxide to biological systems.

Experimental Section

General: Reactions were carried out in oven-dried Schlenk glassware under pure nitrogen when necessary. Solvents were dried with molecular sieves and degassed prior to use. All reagents were purchased either from Sigma–Aldrich or Alfa Aesar and used without further purification. Pentacarbonylmanganese bromide was obtained from Strem Chemicals. 2,2′-Bis(pyrazol-1-yl)ethylamine (bpea),^[58] [Mn(bpea^{N=CHC₆H₄I})(CO)₃]₃PF₆ (**7**),^[46] and [Mn(bpea^{N=CHC₆H₄C=CH})(CO)₃]₃PF₆ (**8**)^[46] were prepared according to published procedures. Azidoacetic acid and Fmoc-(aminoxy)acetic acid were synthesized according to literature methods.^[44,59,60] NMR spectra were recorded with a Bruker DRX 300 spectrometer (¹H: 300.13 MHz; ¹³C: 75.47 MHz) at ambient temperature. Chemical shifts (δ) are given in ppm downfield from tetramethylsilane (TMS) and are referenced to the solvent signal.^[61] Coupling constants *J* are given in Hz. Individual peaks are marked as singlet (s), doublet (d), doublet of doublet (dd), triplet (t), or multiplet (m). Mass spectra were recorded with a Bruker MicroTOF (ESI) instrument; only characteristic fragments are given for the most abundant isotope peak. Data were recorded in positive ion mode. IR spectra were recorded as pure solid samples by using a Nicolet 380 FT-IR Spectrometer equipped with a SMART iTR ATR unit. Elemental analysis (C, H, N) was performed with an EA3000 Elemental Analyser from HEKAtech GmbH, Wegberg. HPLC analysis of the peptides and conjugates was performed with a Dionex Ultimate

3000 instrument equipped with a diode array detector and a ReproSil 100 column (C₁₈, 5 μ m, 4.6 mm for analytical and 10 mm diameter for preparative HPLC, 250 mm length) using a linear gradient of 5–90% acetonitrile/water containing 0.1% TFA as the eluent over 40 min at a flow rate of 0.6 mL min⁻¹ for analytical and 3.0 mL min⁻¹ for preparative chromatography. The myoglobin assay and all photophysical studies were carried out in a quartz cuvette (*d* = 1 cm) with an Agilent 8453 UV/Vis diode array spectrophotometer.

4-({[2,2-Bis(pyrazolyl)ethyl]amino}methyl)benzaldehyde (bpea^{NHCH₂C₆H₄CHO}, **5):** 4-(Diethoxymethyl)benzaldehyde (**2**; 0.58 g, 2.82 mmol) was added to a solution of [2,2-bis(pyrazolyl)ethyl]amine (**1**; 0.50 g, 2.82 mmol) in anhydrous methanol (20 mL). The mixture was heated at reflux in the presence of molecular sieves (4 Å) under nitrogen for 40 h. The molecular sieves were then filtered off, and the solution was cooled to 0 °C to give the intermediate imine **3**. Solid sodium borohydride (186.70 mg, 4.94 mmol) was added to reduce the imine **3**, and stirring was continued for 7 h at room temperature. Water (10 mL) was added to the reaction mixture and the product extracted with dichloromethane (100 mL) and washed with brine (3 × 50 mL). The organic layer was separated, dried with magnesium sulfate (ca. 10 g), and filtered. The solvent was then removed under reduced pressure to give the intermediate aminoacetal **4** as a yellow oil. Yield: 57% (0.60 g, 1.60 mmol). Aminoacetal **4** (0.59 g, 1.60 mmol) was treated with 2 M hydrochloric acid (8 mL) and the mixture stirred at room temperature for 3 h. The reaction mixture turned curdy white, was made alkaline with aqueous sodium hydroxide, and extracted with dichloromethane (3 × 50 mL). The combined organic extracts were washed with brine (3 × 100 mL), dried with sodium sulfate (ca. 10 g), and filtered. The solvent was then removed under reduced pressure to give the product **5** as a yellow oil. Yield: 70% (0.33 g, 1.12 mmol). IR (ATR): $\tilde{\nu}$ = 3115 (m, NH), 2844, 1691 (s, C=O), 1606, 1390, 1090 cm⁻¹. ¹H NMR (300 MHz, CDCl₃): δ = 9.98 (s, 1 H, CHO), 7.82 (d, ³*J* = 8.3 Hz, 2 H, 2,6-H_{Ph}), 7.57 (d, ³*J* = 2.4 Hz, 2 H, 3-H_{Pz}), 7.55 (d, ³*J* = 1.7 Hz, 2 H, 5-H_{Pz}), 7.43 (d, ³*J* = 7.9 Hz, 2 H, 3,5-H_{Ph}), 6.55 [t, ³*J* = 6.9 Hz, 1 H, CH(pz)₂], 6.28 (dd, ³*J* = 2.4, ⁴*J* = 1.8 Hz, 2 H, 4-H_{Pz}), 3.90 (s, 2 H, CH₂C₆H₄) 3.69 (d, ³*J* = 6.9 Hz, 2 H, CH₂-CH) ppm. ¹³C NMR (75.47 MHz, CDCl₃): δ = 51.21 (CH₂CH), 53.03 (CH₂C₆H₄), 75.12 [C(pz)₂], 106.92 (C-4_{Pz}), 128.55 (C-3,5_{Ph}), 129.14 (C-2,6_{Ph}), 130.13 (C-5_{Pz}), 135.66 (C-1_{Ph}), 140.49 (C-3_{Pz}), 147.04 (C-4_{Ph}), 192.07 (CHO) ppm. MS (ESI⁺, MeOH): *m/z* = 318.13 [M + Na]⁺. C₁₆H₁₇N₅O (295.35): C 65.06, H 5.80, N 23.71; found C 64.82, H 5.75, N 23.28.

[Mn(bpea^{NHCH₂C₆H₄CHO})(CO)₃]₃PF₆ (6**):** Pentacarbonylmanganese bromide (368 mg, 1.34 mmol) and bpea^{NHCH₂C₆H₄CHO} (**5**; 346 mg, 1.17 mmol) were dissolved in anhydrous acetone (50 mL) and heated at reflux under nitrogen with the exclusion of light for 5 h. The solvent was removed in vacuo, and the yellow residue was redissolved in methanol (10 mL), and an aqueous solution of potassium hexafluorophosphate (430.70 mg, 2.34 mmol) was added. The yellow product that precipitated was filtered off, washed with water and diethyl ether, and dried under vacuum. Yield: 80% (544.00 mg, 0.94 mmol). IR (ATR): $\tilde{\nu}$ = 3252 (m, N–H), 2036 (s, C=O), 1928 (s, C=O), 1691 (s, CHO), 1607, 1412, 1288, 832 cm⁻¹. ¹H NMR (300 MHz, [D₆]acetone): δ = 10.04 (s, 1 H, CHO), 8.54 (d, ³*J* = 2.2 Hz, 1 H, 3′-H_{Pz}), 8.43 (d, ³*J* = 2.2 Hz, 1 H, 3-H_{Pz}), 8.34 (d, ³*J* = 2.6 Hz, 1 H, 5′-H_{Pz}), 8.28 (d, ³*J* = 2.7 Hz, 1 H, 5-H_{Pz}), 7.93 (d, ³*J* = 8.3 Hz, 2 H, 3,5-H_{Ph}), 7.71 (d, ³*J* = 8.1 Hz, 2 H, 2,6-H_{Ph}), 7.47 [br. s, 1 H, CH(pz)₂], 6.75 (t, ³*J* = 2.4 Hz, 1 H, 4-H_{Pz}), 6.68 (t, ³*J* = 2.4 Hz, 1 H, 4′-H_{Pz}), 5.77 (br. s, 1 H, NH), 4.83 (dd, ³*J* = 13.5, 4.1 Hz, 1 H, CH₂C₆H₄), 4.38 (dd, ³*J* = 13.4, 10.3 Hz, 1 H, CH₂C₆H₄), 3.57 (ddd, ³*J* = 13.2, 7.9, 3.1 Hz, 1 H, CH₂NCH₂C₆H₄),

3.18 (dd, $^3J = 13.8, 8.9$ Hz, 1 H, $\text{CH}_2\text{NCH}_2\text{C}_6\text{H}_4$) ppm. ^{13}C NMR (75.47 MHz, $[\text{D}_6]\text{acetone}$): $\delta = 60.93$ (CH_2N), 72.23 ($\text{CH}_2\text{C}_6\text{H}_4$), 79.28 [$\text{C}(\text{pz})_2$], 118.98 ($\text{C}-4', \text{pz}$), 140.26 ($\text{C}-3, \text{Ph}$), 140.92 ($\text{C}-2, \text{Ph}$), 144.94 ($\text{C}-5', \text{pz}$), 145.42 ($\text{C}-5, \text{pz}$), 147.30 ($\text{C}-4, \text{Ph}$), 152.73 ($\text{C}-1, \text{Ph}$), 157.68 ($\text{C}-3, \text{pz}$), 157.81 ($\text{C}-3', \text{pz}$), 202.23 (CHO) ppm. MS (ESI^+ , MeOH): $m/z = 434.08$ [$\text{M} - \text{PF}_6$] $^+$. $\text{C}_{19}\text{H}_{17}\text{F}_6\text{MnN}_5\text{O}_4\text{P}$ (579.28): calcd. for C 39.39, H 2.95, N 12.09; found C 38.91, H 3.03, N 11.61.

General Conditions for the Solid-Phase Peptide Synthesis (SPPS):

The peptides were synthesized manually in a filter syringe on a 0.39 mmol scale according to the method described by Kirin et al. using the Fmoc strategy.^[62] A preloaded H-L-His(Trt)-2CT resin was used as the solid support. The Fmoc-protected amino acids were deprotected with a solution of 30% piperidine in dmf. For each coupling step, Fmoc-amino acids (5 equiv., 0.97 M in dmf) and coupling reagent (HOBT/HBTU, 0.97 M in dmf) were used. Diisopropylethylamine (DIEA; 10 equiv.) was used as the activator base. The completeness of each coupling step was monitored by the Kaiser test.^[63] The final coupling of 5-hexynoic acid, azidoacetic acid, and (aminoxy)acetic acid was performed by using a solution of 5-hexynoic acid/HOBT/HBTU, azidoacetic acid/HOBT/HBTU or Fmoc-(aminoxy)acetic acid/HOBT/HBTU in dmf with DIEA as activator base over 2 h. The peptide was cleaved from the solid support manually in a filter syringe at room temperature using a cleavage cocktail of TFA/TIS/ H_2O (90:5:5). The peptide was then isolated by precipitation with cold diethyl ether (-25°C) and repeated cycles of washing, centrifuging, and decanting. The residue was then dissolved in acetonitrile/water (1:1, v/v) and lyophilized to yield the peptides as white solids.

$\text{HC}\equiv\text{C}(\text{CH}_2)_3\text{CO}-\text{Leu}-\text{Pro}-\text{Leu}-\text{Gly}-\text{Asn}-\text{Ser}-\text{His}-\text{OH}$ (9): Peptide **9** was synthesized on a 0.24 mmol scale on preloaded H-L-His(Trt)-2CT resin (300 mg, 0.78 mmol g^{-1}) by using the amino acids Fmoc-L-Ser(*t*Bu)-OH, Fmoc-L-Asn(Trt)-OH, Fmoc-L-Gly-OH, Fmoc-L-Leu-OH, Fmoc-L-Pro-OH, and Fmoc-L-Leu-OH under manual solid-phase peptide synthesis conditions as described above. Two repeated couplings of 5-hexynoic acid (10 equiv.) were required to attain complete coupling, as indicated by a negative Kaiser test. Cleavage time: 3 h with TFA/TIS/ H_2O (90:5:5, v/v). The peptide was obtained as a white solid. Yield: 54% (106 mg, 0.13 mmol). RP-HPLC: $t_r = 22.80$ min. MS (ESI^+ , MeOH): $m/z = 831.43$ [$\text{M} + \text{H}$] $^+$. IR (ATR): $\tilde{\nu} = 3290$ (m), 2959 (m), 1659 (s), 1623 (s), 1538 (s), 1437 (m), 1197 (s), 1134 (s) cm^{-1} .

$\text{N}_3\text{-Ac}-\text{Leu}-\text{Pro}-\text{Leu}-\text{Gly}-\text{Asn}-\text{Ser}-\text{His}-\text{OH}$ ($\text{N}_3\text{-Ac}-\text{TGF}\beta_1\text{-OH}$, 10): Peptide **10** was synthesized on a 0.39 mmol scale on preloaded H-L-His(Trt)-2CT resin (500 mg, 0.78 mmol g^{-1}) by using the amino acids Fmoc-L-Ser(*t*Bu)-OH, Fmoc-L-Asn(Trt)-OH, Fmoc-L-Gly-OH, Fmoc-L-Leu-OH, Fmoc-L-Pro-OH, and Fmoc-L-Leu-OH under manual solid-phase peptide synthesis conditions as described above. Two repeated couplings of azidoacetic acid (10 equiv.) were required to attain complete coupling, as indicated by a negative Kaiser test. Cleavage time: 3 h with TFA/TIS/ H_2O (90:5:5, v/v). The peptide was obtained as a white solid. Yield: 55% (172 mg, 0.21 mmol). RP-HPLC: $t_r = 22.90$ min. MS (ESI^+ , MeOH): $m/z = 820.40$ [$\text{M} + \text{H}$] $^+$. IR (ATR): $\tilde{\nu} = 3284$ (m), 2958 (m), 2109 (s, N_3) 1658 (s), 1536 (s), 1440 (m), 1200 (s), 1134 (s) cm^{-1} .

Aoa-Leu-Pro-Leu-Gly-Asn-Ser-His-OH (Aoa-TGF β_1 -OH, 11): Peptide **11** was synthesized on a 0.319 mmol scale on preloaded H-L-His(Trt)-2CT resin (500 mg, 0.78 mmol g^{-1}) by using the amino acids Fmoc-L-Ser(*t*Bu)-OH, Fmoc-L-Asn(Trt)-OH, Fmoc-L-Gly-OH, Fmoc-L-Leu-OH, Fmoc-L-Pro-OH, and Fmoc-L-Leu-OH under manual solid-phase peptide synthesis conditions as described above. Two repeated couplings of Fmoc-Aoa-OH (10 equiv.) were

required to attain complete coupling, as indicated by a negative Kaiser test. Cleavage time: 3 h with TFA/TIS/ H_2O (90:5:5, v/v). The peptide was obtained as a white solid. Yield: 60% (185 mg, 0.23 mmol). RP-HPLC: $t_r = 15.60$ min. MS (ESI^+ , MeOH): $m/z = 810.41$ [$\text{M} + \text{H}$] $^+$. IR (ATR): $\tilde{\nu} = 3288$ (m), 2961 (m), 1658 (s), 1537 (s), 1439 (m), 1198 (s), 1133 (s) cm^{-1} .

[Mn(bpea $^{\text{C}\equiv\text{C}(\text{CH}_2)_3\text{CO}-\text{TGF}\beta_1\text{-OH}$)(CO) $_3$]PF $_6$ (12): [Mn(bpea $^{\text{N}=\text{CHC}_6\text{H}_4\text{I}}$)(CO) $_3$]PF $_6$ (**7**; 24.30 mg, 36 μmol) and the peptide 5-hexynoic-TGF β_1 -OH (**9**; 30 mg, 36 μmol) were dissolved in dmf (1 mL) and triethylamine (1.5 mL), and the solution was degassed by three freeze-pump-thaw cycles. Copper(I) iodide (1 mg, 4.32 μmol , 12 mol-%) and *cis*-dichlorobis(triphenylphosphine)palladium(II) (1 mg, 1.44 μmol , 4 mol-%) were added under nitrogen, and the reaction mixture was degassed. The yellow solution was stirred at room temperature under the exclusion of light for 28 h and then loaded onto a short reversed-phase column (Waters C $_{18}$ Sep-Pak, 5 g) washed with water (5×10 mL). However, no conjugate formation could be detected under these conditions as probed by HPLC and ESI-MS.

[Mn(bpea $^{\text{C}_2\text{HN}_3-\text{CH}_2\text{CO}-\text{TGF}\beta_1\text{-OH}$)(CO) $_3$]PF $_6$ (13): [Mn-(bpea $^{\text{N}=\text{CHC}_6\text{H}_4\text{C}\equiv\text{CH}}$)(CO) $_3$]PF $_6$ (**8**; 28.02 mg, 48.90 μmol) and the peptide $\text{N}_3\text{-Ac}-\text{TGF}\beta_1\text{-OH}$ (**10**; 40.10 mg, 48.90 μmol) were dissolved in dmf/water (1:1, v/v, 2 mL). Sodium ascorbate (0.70 mg, 3.50 μmol , 25 mol-%) and copper(II) sulfate pentahydrate (0.15 mg, 0.70 μmol , 5 mol-%) were subsequently added, and the mixture was stirred at room temperature under the exclusion of light for 24 h. The yellow solution was loaded onto a short reversed-phase column (Waters C $_{18}$ -SepPak, 5 g) washed with water (5×10 mL). The conjugate was then eluted with acetonitrile as a yellow band. The solution was lyophilized to give the product as a yellow solid. Yield: 20% (13 mg, 9.50 μmol). RP-HPLC: $t_r = 30.10$ min. MS (ESI^+ , MeOH): $m/z = 1247.45$ [$\text{M} - \text{PF}_6$] $^+$. IR (ATR): $\tilde{\nu} = 2958$ (m), 2040 (s, $\text{C}\equiv\text{O}$), 1932 (s, $\text{C}\equiv\text{O}$), 1663 (s), 1533 (m), 1413 (m), 1132 (m) cm^{-1} .

[Mn(bpea $^{\text{NHCH}_2\text{C}_6\text{H}_4\text{CH}=\text{OCH}_2\text{CO}-\text{TGF}\beta_1\text{-OH}$)(CO) $_3$]PF $_6$ (14): Complex [Mn(bpea $^{\text{NHCH}_2\text{C}_6\text{H}_4\text{CHO}}$)(CO) $_3$]PF $_6$ (**6**; 5.79 mg, 0.01 mmol) and the peptide Aoa-TGF β_1 -OH (**11**; 10 mg, 0.01 mmol) were dissolved in a 1:1 (v/v) mixture of tetrahydrofuran (2 mL) and phosphate buffer saline (PBS; 2 mL, 100 mM, pH 5.2). The resulting yellow solution was stirred at room temperature under the exclusion of light for 3 h. The solvent was removed by lyophilization, and the yellow residue was dissolved in acetonitrile/water (1:9, v/v) and loaded onto a short reversed-phase column (Waters C $_{18}$ -SepPak, 5 g) washed with water (5×10 mL) followed by acetonitrile (5×10 mL). The conjugate was then eluted with acetonitrile/water (1:1, v/v) as a yellow band. The solution was lyophilized to give the product as a yellow solid. Yield: 58% (8 mg, 0.006 mmol). RP-HPLC: $t_r = 28.30$ min. MS (ESI^+ , MeOH): $m/z = 1225.45$ [$\text{M} - \text{PF}_6$] $^+$. IR (ATR): $\tilde{\nu} = 3284$ (m), 2042 (s, $\text{C}\equiv\text{O}$), 1934 (s, $\text{C}\equiv\text{O}$), 1662 (s), 1546 (s), 1413 (m), 1195 (s), 1132 (s) cm^{-1} .

Myoglobin Assay:^[51,52] In a quartz cuvette, a solution of horse skeletal muscle myoglobin (576 μL , 60 μM) in 0.1 M phosphate buffer (PBS, pH 7.4) was degassed by bubbling with nitrogen and reduced by the addition of sodium dithionite (10 mM, 100 μL) in PBS buffer (0.1 M, pH 7.4) to a total volume of 676 μL for **6** and 795 μL for **14**. Compound **6** or **14** in dimethyl sulfoxide (10 μL , 15 μM each) was added to this solution, followed by PBS to give a total volume of 1000 μL with final concentrations of 15 μM of **6**, 15 μM of **14**, 10 mM of sodium dithionite, and 60 μM of myoglobin with $A_{557} < 1$. The solutions were freshly prepared for both the dark-stability measurements and the photoillumination experiments. Illuminations were carried out under nitrogen at 365 nm with a UV hand

lamp (6 W, UVITEC, UK) positioned perpendicular to the cuvette at a distance of 3 cm. Illuminations were interrupted at regular intervals of 5 min for the initial 60 min and then at 10 min intervals to record UV/Vis spectra with an Agilent 8453 UV/Vis diode array spectrophotometer. As a dark control, measurements were carried out by using the automated spectrometer software for a defined period of time (16 h). All the illumination experiments were carried out in triplicate.

Ferrioxalate Actinometry: Ferrioxalate actinometry was used to determine the photon flux of the 365 nm UV hand lamp because of its sensitivity, wide spectral range, including the ultraviolet, and ease of use.^[64,65] The whole ferrioxalate actinometry procedure, including the preparation of solutions, was carried out under red safe-light. The number of moles of ferrous iron formed was determined spectrophotometrically by complexation with 1,10-phenanthroline (phen) to give the colored tris(phenanthroline) complex $[\text{Fe}(\text{phen})_3]^{2+}$ with $\lambda_{\text{max}} = 510$ nm. In a 1 cm quartz cell, 0.006 M (3 mL) of potassium ferrioxalate in 0.05 M sulfuric acid as the chemical actinometer was irradiated with a 365 nm UV hand lamp under efficient stirring. This irradiated solution (1 mL) was mixed with 0.1% 1,10-phenanthroline in water and sodium acetate buffer (0.5 mL) in water (1 M, pH 3.5) and further diluted to 10 mL with water. A reference was prepared in the same way except that it was not irradiated. Both solutions were placed in the dark (about 1 h) to allow complexation to complete. The absorbance was then measured at 510 nm ($\epsilon = 11100 \text{ M}^{-1} \text{ cm}^{-1}$). A_{510} was maintained within the range of 0.4–1.0. The photon flux of the 365 nm UV hand lamp was then calculated by using the following equation with $\Phi_{365 \text{ nm}} = 1.21$, $V_1 =$ volume of potassium ferrioxalate illuminated, $V_2 =$ volume of V_1 used for complexation with 1,10-phenanthroline, $V_3 =$ total volume:^[66]

$$\Phi_p = \frac{10^{-3} \Delta A V_1 V_3}{\Phi_{\lambda} \epsilon_{510} V_2 t}$$

X-ray Crystallography: A single crystal of **6** was immersed in a film of perfluoropolyether oil, mounted on a glass fiber, and transferred to the diffractometer in a stream of cold nitrogen. Diffraction data were collected with a Bruker D8 Quest diffractometer at 100 K using graphite-monochromated Mo- K_{α} radiation ($\lambda = 0.71073 \text{ \AA}$). Final cell constants were obtained from a least-squares fit of a subset of a few thousand strong reflections. The APEX2 program (ver. 2012.4-3, Bruker AXS) package was used for data collection, the SAINT-PLUS software (ver. 8.18C, Bruker AXS) for cell refinement and data reduction, SADABS 2008/1 (Bruker 2008) to account for the absorption, and SHELXL-97 for refinement and drawing of the structures. CCDC-956477 contains the supplementary crystallographic data for this paper. These data can be obtained free of charge from The Cambridge Crystallographic Data Centre via www.ccdc.cam.ac.uk/data_request/cif.

Supporting Information (see footnote on the first page of this article): ^1H NMR spectrum of compound **6**, ESI mass spectra of **6**, **10**, and **13**, IR spectra of **13** and **14**, and UV/Vis spectra and CO release data for **6** and **14**.

Acknowledgments

This work was supported by the Deutsche Forschungsgemeinschaft (DFG) within the project FOR 630 “Biological function of organometallic compounds”.

- [1] T. Matsui, M. Unno, M. Ikeda-Saito, *Acc. Chem. Res.* **2010**, *43*, 240–247.
 [2] M. D. Maines, *Ann. Rev. Pharmacol. Toxicol.* **1997**, *37*, 517–554.

- [3] L. Wu, R. Wang, *Pharmacol. Rev.* **2005**, *57*, 585–630.
 [4] C. A. Piantadosi, *Free Radiat. Biol. Med.* **2008**, *45*, 562–569.
 [5] N. G. Abraham, A. Kappas, *Pharmacol. Rev.* **2008**, *60*, 79–127.
 [6] R. Motterlini, J. E. Clark, R. Foresti, P. Sarathchandra, B. E. Mann, C. J. Green, *Circ. Res.* **2002**, *90*, e17–e24.
 [7] R. Alberto, R. Motterlini, *Dalton Trans.* **2007**, 1651–1660.
 [8] R. Motterlini, L. E. Otterbein, *Nature Rev. Drug Discovery* **2010**, *9*, 728–743.
 [9] B. E. Mann in *Topics in Organometallic Chemistry*, vol. 32 (Eds.: N. Metzler-Nolte, G. Jaouen), Springer, Berlin, **2010**, pp. 247–285.
 [10] B. E. Mann, *Organometallics* **2012**, *31*, 5728–5735.
 [11] F. Zobi, *Future Med. Chem.* **2013**, *5*, 175–188.
 [12] T. R. Johnson, B. E. Mann, I. P. Teasdale, H. Adams, R. Foresti, C. J. Green, R. Motterlini, *Dalton Trans.* **2007**, 1500–1508.
 [13] S. Romanski, B. Kraus, U. Schatzschneider, J. Neudörfl, S. Amslinger, H.-G. Schmalz, *Angew. Chem. Int. Ed.* **2011**, *50*, 2392–2396; *Angew. Chem.* **2011**, *123*, 2440.
 [14] S. Romanski, B. Kraus, M. Guttentag, W. Schlundt, H. Rücker, A. Adler, J.-M. Neudörfl, R. Alberto, S. Amslinger, H.-G. Schmalz, *Dalton Trans.* **2012**, *41*, 13862–13875.
 [15] S. Botov, E. Stamellou, S. Romanski, M. Guttentag, R. Alberto, J. Neudörfl, B. Yard, H.-G. Schmalz, *Organometallics* **2013**, *32*, 3587–3594.
 [16] S. Romanski, H. Rücker, E. Stamellou, M. Guttentag, J. Neudörfl, R. Alberto, S. Amslinger, B. Yard, H.-G. Schmalz, *Organometallics* **2012**, *31*, 5800–5809.
 [17] P. C. Kunz, H. Meyer, J. Barthel, S. Sollazzo, A. M. Schmidt, C. Janiak, *Chem. Commun.* **2013**, *49*, 4896–4898.
 [18] U. Schatzschneider, *Eur. J. Inorg. Chem.* **2010**, 1451–1467.
 [19] U. Schatzschneider, *Inorg. Chim. Acta* **2011**, *374*, 19–23.
 [20] R. D. Rimmer, A. E. Pierri, P. C. Ford, *Coord. Chem. Rev.* **2012**, *256*, 1509–1519.
 [21] P. V. Simpson, U. Schatzschneider in *Inorganic Chemical Biology: Principles, Techniques and Applications* (Ed.: G. Gasser), Wiley, Chichester, **2014**.
 [22] C. C. Romao, W. A. Blättler, J. D. Seixas, G. J. L. Bernardes, *Chem. Soc. Rev.* **2012**, *41*, 3571–3583.
 [23] A. R. Marques, L. Kromer, D. J. Gallo, N. Penacho, S. S. Rodrigues, J. D. Seixas, G. J. L. Bernardes, P. M. Reis, S. L. Otterbein, R. A. Ruggieri, A. S. G. Goncalves, A. M. L. Goncalves, M. N. De Matos, I. Bento, L. E. Otterbein, W. A. Blättler, C. C. Romao, *Organometallics* **2012**, *31*, 5810–5822.
 [24] U. Hasegawa, A. J. van der Vlies, E. Simeoni, C. Wandrey, J. A. Hubbell, *J. Am. Chem. Soc.* **2010**, *132*, 18273–18280.
 [25] M. Ma, H. Noei, B. Mienert, J. Niesel, E. Bill, M. Muhler, R. A. Fischer, Y. Wang, U. Schatzschneider, N. Metzler-Nolte, *Chem. Eur. J.* **2013**, *19*, 6785–6790.
 [26] G. Dördelmann, T. Meinhardt, T. Sowik, A. Krüger, U. Schatzschneider, *Chem. Commun.* **2012**, *48*, 11528–11530.
 [27] G. Dördelmann, H. Pfeiffer, A. Birkner, U. Schatzschneider, *Inorg. Chem.* **2011**, *50*, 4362–4367.
 [28] J. B. Matson, M. J. Webber, V. K. Tamboli, B. Weber, S. I. Stupp, *Soft Matter* **2012**, *8*, 6689–6692.
 [29] P. S. Kabouridis, *Trends Biotechnol.* **2003**, *21*, 498–503.
 [30] I. Neundorf, J. Hoyer, K. Splith, R. Rennert, H. W. Peindy N’Dongo, U. Schatzschneider, *Chem. Commun.* **2008**, 5604–5606.
 [31] H. W. Peindy N’Dongo, I. Neundorf, K. Merz, U. Schatzschneider, *J. Inorg. Biochem.* **2008**, *102*, 2114–2119.
 [32] H. W. Peindy N’Dongo, I. Ott, R. Gust, U. Schatzschneider, *J. Organomet. Chem.* **2009**, *694*, 823–827.
 [33] K. Splith, W. Hu, U. Schatzschneider, R. Gust, I. Ott, L. A. Onambele, A. Prokop, I. Neundorf, *Bioconjugate Chem.* **2010**, *21*, 1288–1296.
 [34] K. Splith, I. Neundorf, W. Hu, H. W. Peindy N’Dongo, V. Vasylyeva, K. Merz, U. Schatzschneider, *Dalton Trans.* **2010**, *39*, 2536–2545.
 [35] J. Hoyer, U. Schatzschneider, M. Schulz-Siegmund, I. Neundorf, *Beilstein J. Org. Chem.* **2012**, *8*, 1788–1797.

- [36] W. Hu, K. Splith, I. Neundorf, K. Merz, U. Schatzschneider, *J. Biol. Inorg. Chem.* **2012**, *17*, 175–185.
- [37] C. R. Bertozzi, E. M. Sletten, *Angew. Chem. Int. Ed.* **2009**, *48*, 6974–6998; *Angew. Chem.* **2009**, *121*, 7108.
- [38] R. K. V. Lim, Q. Lin, *Chem. Commun.* **2010**, *46*, 1589–1600.
- [39] M. Boyce, C. R. Bertozzi, *Nature Methods* **2011**, *8*, 638–642.
- [40] C. P. Ramil, Q. Lin, *Chem. Commun.* **2013**, *49*, 11007–11022.
- [41] H. Pfeiffer, A. Rojas, J. Niesel, U. Schatzschneider, *Dalton Trans.* **2009**, 4292–4298.
- [42] J. B. Yue, K. M. Mulder, *Pharmacol. Ther.* **2001**, *91*, 1–34.
- [43] A. Dirksen, P. E. Dawson, *Bioconjugate Chem.* **2008**, *19*, 2543–2548.
- [44] H. Pfeiffer, T. Sowik, U. Schatzschneider, *J. Organomet. Chem.* **2013**, *734*, 17–24.
- [45] S. Ulrich, D. Boturyn, A. Marra, O. Renaudet, P. Dumy, *Chem. Eur. J.* **2014**, *20*, 34–41.
- [46] S. Pai, M. Hafftilang, G. Atongo, C. Nagel, J. Niesel, S. Botov, H.-G. Schmalz, B. Yard, U. Schatzschneider, *Dalton Trans.* **2014**, DOI: 10.1039/c1034dt00254g.
- [47] J. J. J. M. Donners, G. A. Silva, H. A. Behanna, S. G. Anthony, Northwestern University, US Pat. 7544661 B2, **2009**.
- [48] R. Chinchilla, C. Nájera, *Chem. Rev.* **2007**, *107*, 874–922.
- [49] H. Pfeiffer, A. Rojas, J. Niesel, U. Schatzschneider, *Dalton Trans.* **2009**, 4292–4298.
- [50] R. Chinchilla, C. Najera, *Chem. Soc. Rev.* **2011**, *40*, 5084–5121.
- [51] A. J. Atkin, J. M. Lynam, B. E. Moulton, P. Sawle, R. Motterlini, N. M. Boyle, M. T. Pryce, I. J. S. Fairlamb, *Dalton Trans.* **2011**, *40*, 5755–5761.
- [52] S. McLean, B. E. Mann, R. K. Poole, *Anal. Biochem.* **2012**, *427*, 36–40.
- [53] R. D. Rimmer, H. Richter, P. C. Ford, *Inorg. Chem.* **2009**, *48*, 1180–1185.
- [54] M. A. Gonzalez, M. A. Yim, S. Cheng, A. Moyes, A. J. Hobbs, P. K. Mascharak, *Inorg. Chem.* **2011**, *50*, 601–608.
- [55] M. A. Gonzalez, S. J. Carrington, N. L. Fry, J. L. Martinez, P. K. Mascharak, *Inorg. Chem.* **2012**, *51*, 11930–11940.
- [56] P. Govender, S. Pai, U. Schatzschneider, G. Smith, *Inorg. Chem.* **2013**, *52*, 5470–5478.
- [57] C. Bischof, A. Dimri, T. Joshi, S. Pai, L. Spiccia, U. Schatzschneider, *Inorg. Chem.* **2013**, *52*, 9297–9308.
- [58] D. L. Reger, B. Reinecke, M. D. Smith, R. F. Semeniuc, *Inorg. Chim. Acta* **2009**, *362*, 4377–4388.
- [59] J. Cai, X. Li, X. Yue, J. S. Taylor, *J. Am. Chem. Soc.* **2004**, *126*, 16324–16325.
- [60] M. H. Lott, *J. Am. Chem. Soc.* **1948**, *70*, 1972.
- [61] G. R. Fulmer, A. J. M. Miller, N. H. Sherden, H. E. Gottlieb, A. Nudelman, B. M. Stoltz, J. E. Bercaw, K. I. Goldberg, *Organometallics* **2010**, *29*, 2176–2179.
- [62] S. I. Kirin, F. Noor, N. Metzler-Nolte, W. Mier, *J. Chem. Educ.* **2007**, *84*, 108–111.
- [63] E. Kaiser, R. L. Colescott, C. D. Bossinger, P. I. Cook, *Anal. Biochem.* **1970**, *34*, 595–598.
- [64] C. A. Parker, *Proc. R. Soc. London, Ser. A* **1953**, *220*, 104–116.
- [65] C. G. Hatchard, C. A. Parker, *Proc. R. Soc. London, Ser. A* **1956**, *235*, 518–536.
- [66] H. J. Kuhn, S. E. Braslavskyi, R. Schmidt, *Pure Appl. Chem.* **1989**, *61*, 187–210.

Received: February 28, 2014
Published Online: May 16, 2014